BUILDING EXTRACTION FROM MULTIPLE DATA SOURCES: A DATA FUSION FRAMEWORK FOR RECONSTRUCTION OF GENERIC MODELS

K. Khoshelham

Dept. of Land Surveying and Geo-Informatics, The Hong Kong Polytechnic University, Hong Kong
Kourosh.k@polyu.edu.hk

Commission III, WG III/4

KEY WORDS: Building Extraction, Fusion, Automation, Modelling, Aerial image, Laser scanning, GIS

ABSTRACT:

Automated building extraction from multi-source data has attracted great attention in recent years. This paper presents an approach to automated building extraction by fusion of image data, height data and 2D ground plans. In this approach buildings are detected using ground plans and height data. A split-and-merge process is applied to fuse image and height data and derive the parametric forms of roof planes. Vegetation regions are identified and discarded using the image information in red and infrared channels. Walls are reconstructed as vertical planes upon the ground plan. The model planar faces are finally intersected and resulting plane patches are assembled together to form a generic polyhedral model. Results of the experimental testing indicate the promising performance of the proposed approach in automatic detection and reconstruction of buildings.

1. INTRODUCTION

Automated building extraction has been a challenging problem in the past two decades. Automated approaches that work solely based on a single source of data, suffer from the lack of robustness due to complexities in data as well as in buildings. Therefore, in recent years research efforts have been focused on automated approaches that make use of data from multiple sources. This paper presents a framework for fusion of available data sources that can be used in an automated system for extraction of building objects.

Various types of data from different sources have been used for automated extraction of buildings. Aerial images are the most widely used data. Single aerial images have been used for automated detection and reconstruction of buildings with simple models (Huertas et al., 1993; Lin et al., 1995; Lin and Nevatia, 1996; Nevatia et al., 1997; Shufelt and McKeown, 1993). For reconstruction of more complex buildings, stereo and multiple overlap aerial images have attracted greater attention (Baillard et al., 1999; Bignone et al., 1996; Dang et al., 1994; Fischer et al., 1998; Fua and Hanson, 1991; Henricsson, 1998; Henricsson and Baltsavias, 1997; Herman and Kanade, 1986; Jaynes et al., 2003; Kolbe, 1999; Moons et al., 1998). Image data from other sources have not been suitable for building reconstruction. Remotely sensed images from satellites are of relatively low ground resolution and, therefore, can only be used for detection of buildings. Close range images are, on the other hand, too detailed and can be used to map textures onto final reconstructed models.

Height data is another widely used type of data. Digital surface models (DSMs) from aerial laser scanning systems have been used in a number of approaches (Brunn and Weidner, 1997; Maas, 1999; Vosselman, 1999; Weidner and Forstner, 1995). Range data from terrestrial laser scanners, however, has not been proved useful for automated building extraction.

Automated building extraction from both image and height data encounters a number of complexities. Image data often suffers from noise, low contrast, shadow and occlusion; hence, features extracted from images are incomplete and uncertain. Height data is of relatively low resolution, which makes the extraction of building boundaries difficult. These complexities have led the research efforts toward methods that combine data from multiple sources. In recent years a number of methods have been developed for fusion of image and height data (Ameri, 2000; Cord et al., 2001; Jaynes et al., 2003; Rottensteiner and Jansa, 2002), although height data in some of these methods has been generated from image data using matching techniques. Fusion of image data and 2D ground plans has also appeared in a number of works (Haala and Anders, 1996; Jibrini et al., 2000; Pasko and Gruber, 1996; Suveg and Vosselman, 2004). In another fusion strategy, Haala and Brenner (1998) used DSM and 2D ground plans in an approach to automated building extraction.

Despite the great deal of research that has been carried out on automated building extraction, still the role of multi-source data and fusion strategies has not been completely explored. The objective of this paper is to develop a framework for fusion of available data sources that can be used for automated extraction of buildings. The proposed fusion framework combines aerial images in colour and infrared channels, DSM and DTM from aerial laser scanner and 2D ground plans from a GIS database in an approach to automated extraction of buildings. In this approach ground plans are used to detect buildings in the scene and reconstruct the walls. Image data in red and infrared channels are used to identify and remove vegetation regions. Roof planes are reconstructed by exploiting information from image, DSM and DTM. Generic polyhedral models are finally formed by assembling reconstructed walls and roof planes.

The paper is structured in 6 sections. In section 2 an overview of the proposed fusion strategy is presented. Reconstruction of walls and roof planes are described in section 3. Section 4 discusses the reconstruction of generic models using a plane patch reconstruction technique. Experiments and results are shown in section 5. Conclusions are made in section 6.

2. A FRAMEWORK FOR FUSION OF IMAGE DATA, HEIGHT DATA AND 2D GROUND PLANS

The first step in a building extraction system is the detection of buildings in the scene. In this work, buildings are detected by projecting ground plans to image data. For this purpose, the third dimension (height) of the ground plans is interpolated in the height data.

Having buildings detected in the scene, the reconstruction part is based on finding parametric forms of the model planar faces. These planar faces are then intersected and resulting plane patches are assembled together to form a generic polyhedral model. Roof planes are reconstructed by fusion of image and height data through a split-and-merge process. This process starts with segmenting the image data within the localized areas. Height points from the DSM are projected to extracted image regions and a robust regression method is employed to fit planar faces to height points belonging to each image region. Regions in which more than a single plane is detected are split and neighbouring regions whose planes are coplanar are merged. Vegetation regions are identified and discarded by computing an NDVI measure derived from red and infrared channels. Every planar face is attributed based on its slope and height over the DTM. A planar face is attributed as non-roof if its height over the DTM is smaller than a minimum tolerance; otherwise it is attributed as flat roof if its largest slope is smaller than a slope threshold or as slanted roof if the largest slope is larger than the slope threshold.

Wall faces are obtained by reconstructing a vertical wall over every line segment of the 2D ground plan. The average terrain height, derived from DTM, defines the planar surface that lies beneath the building. After the parametric forms of all planar faces of the building are computed, every three planar faces are intersected and the resulting vertex is verified to make sure it is a correct model vertex. Verified vertices of each planar face are sorted in order to form a planar patch. Planar patches form the final generic polyhedral model that can be visualized using a graphical engine.

The basic assumption in this approach is that buildings are formed by planar faces and that walls are vertical. In addition, building roofs are assumed to be one of the following three types: flat roof, gable roof and hipped roof. In other words this approach aims for reconstructing simple building types using a boundary-representation (B-Rep) modelling scheme. Nevertheless, more complex buildings such as buildings with cross-gabled roofs can still be reconstructed by adopting a Constructive Solid Geometry (CSG) modelling scheme. In this way, similar to the method developed by Suveg and Vosselman (2004), the 2D ground plan is first partitioned into rectangular parts where each part is reconstructed using the plane patch reconstruction method described above. These building parts are then combined together to form the final generic model.

3. RECONSTRUCTION OF PARAMETRIC FORMS OF THE MODEL PLANAR FACES

Buildings are localized in the image using ground plans and height data. A split-and-merge process is applied to fuse image and height data in the localized areas and derive the parametric forms of roof planes. Walls are reconstructed by finding the parametric forms of vertical planes built on the ground plan. The following sections describe the above processes in more details.

3.1 Localization of buildings using ground plans and height data

A 2D ground plan is usually stored as a polygon with an array of corner points with X and Y coordinates in the world coordinate system. The footprint of each building is localized in the image by interpolating the height of every corner point of the ground plan in DTM and projecting the resulting 3D corner points to the image. Interpolation of heights in DSM with the same procedure helps to find roof boundaries of the building in the image assuming that walls are vertical and there is no eave overshooting. Concatenation of these two polygons (footprint and roof boundary) defines the actual area where the building appears in the image.

3.2 Reconstruction of roof planes using image and height data

Reconstruction of roof planes is based on image regions extracted in areas where building candidates are detected. Extraction of image regions is carried out using watershed segmentation algorithm (Vincent and Soille, 1991). Extended minima transform (Soille, 1999) is employed to control excessive oversegmentation.

While a desirable segmentation is a partitioning of the image into regions where each region corresponds to a single planar face in object space, segmentation algorithms often result in undergrown and/or overgrown regions. The purpose of the split-and-merge process is to refine the result of initial segmentation by making use of clues derived from the DSM. For this purpose, height points are projected from DSM to extracted image regions and a robust regression method is used to fit planar faces to height points belonging to each image region. This method is based on random selection of a finite set of samples from data (trial estimates) (Fischler and Bolles, 1981). Least median of squared residuals (Rousseeuw and Leroy, 1987) is used to find the best sample and also outlier points. Each sample contains three data points randomly selected from the DSM. These points define a plane. For other points a residual value is calculated as to how they fit into this plane. The sample with the least median of squared residuals is selected for outlier detection. Outliers are detected as points with residuals larger than a predefined tolerance and are treated as a new dataset to determine whether they fit into a new plane. The plane fitting process is iterated until no more planes can be fitted to data points.

After planar faces are detected in each image region, the segmented image is searched for regions in which more than one plane is detected. Those regions are overgrown regions; hence, they are split into two or more regions depending on the number of detected planes. To detect and merge undergrown regions, first a region adjacency graph is constructed by tracking region boundaries in the segmented image. Plane parameters of every two neighbouring regions enter a coplanarity check and the two neighbouring regions are merged if their associated planes are coplanar.

An example of the performance of the split-and-merge process is demonstrates in figure 1. As can be seen in figure 1(B), the initial segmentation results in an overgrown and an undergrown region in the right part of the roof. The result of the split-and-merge process is shown in figure 1(C) where the overgrown region is split and two undergrown regions are merged to form a correct roof region.
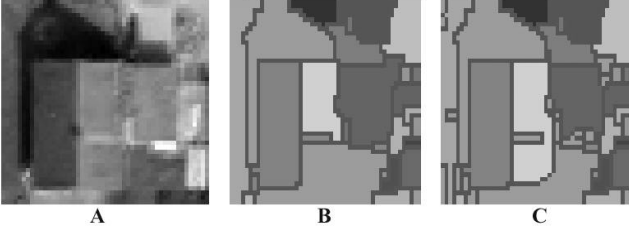
Figure 1: The split-and-merge process: A. The original image; B. The initial segmentation; C. The result of the split-and-merge process.

The result of the split-and-merge process is more likely to be a correct partitioning of the image where each region associates with a single surface in object space. However, planar faces might have been detected also in vegetation regions. To avoid the influence of vegetation, image data in red and near infrared channel is used to identify and discard vegetation regions. For this purpose a normalized difference vegetation index (NDVI) is computed for each pixel from the following equation:

$$NDVI = \frac{NIR - RED}{NIR + RED} \qquad (1)$$

where *NIR* and *RED* denote pixel values in near infrared and red channels respectively. NDVI is related to the proportion of photosynthetically absorbed radiation and its value varies from –1 to +1. Vegetation is characterized by high NDVI value and a region is identified as a vegetated region if at least 70% of its pixels are vegetation pixels.

To determine the final roof planes among the remaining regions the difference between DSM height and DTM height for height points belonging to each region is used. A planar surface is attributed as non-roof if the difference between its average DSM height and DTM height is smaller than a minimum threshold; otherwise it is attributed as flat-roof if its largest slope is smaller than a slope threshold or as slanted-roof if the largest slope is larger than the slope threshold.

3.3 Reconstruction of vertical walls upon ground plans

The parametric form of a plane passing through a point $p = (x_p, y_p, z_p)^T$ and perpendicular to a normal vector $n = (a_1, a_2, a_3)^T$ can be written as:

$$a_1 x + a_2 y + a_3 z = k \qquad (2)$$

where:

$$k = a_1 x_p + a_2 y_p + a_3 z_p \qquad (3)$$

For a vertical plane $a_3 = 0$ and the plane equation becomes:

$$a_1 x + a_2 y = k \qquad (4)$$

where:

$$k = a_1 x_p + a_2 y_p$$

Therefore, each line segment of the ground plan with endpoints $p_1 = (x_1, y_1)^T$, $p_2 = (x_2, y_2)^T$ can solve for a_1, a_2 and define a vertical plane as follows:

$$a_1 x + a_2 y + a_3 z + a_4 = 0$$

$$where:$$
$$a_1 = y_1 - y \qquad (5)$$
$$a_2 = x_2 - x_1$$
$$a_3 = 0$$
$$a_4 = x_1 y_2 - x_2 y_1$$

Parameters of the reconstructed wall faces are stored along with two endpoints used in the calculations. Wall faces and planar roof faces computed in the split-and-merge process enter the plane patch reconstruction procedure described below.

4. RECONSTRUCTION OF PLANE PATCHES

A plane patch is defined as a planar polygon in 3D space. So far, the computed model faces are represented in parametric form. For graphical visualization, however, one requires plane patches, which are represented by their vertices. Reconstruction of plane patches is carried out in three steps: plane intersection, verification of vertices and sorting of vertices. In the following these steps are described in more details.

4.1 Plane intersection

Two planes in 3D space intersect in a line if they are not parallel or coplanar. This line will intersect a third plane in one point if it is not parallel to it and does not lie in it. Therefore, in regular case three planes in 3D space intersect in a point if they are not in a special relation to each other. In algebraic form, a system of three equations of the form denoted in eq. 2 has exactly one solution if the equations are linearly independent. More precisely if normal vectors of the three planes are linearly independent then equations of the planes form a regular system of three equations and three unknowns as denoted in eq. 6:

$$a_{11} x + a_{12} y + a_{13} z = k_1$$
$$a_{21} x + a_{22} y + a_{23} z = k_2 \qquad (6)$$
$$a_{31} x + a_{32} y + a_{33} z = k_3$$

where a_{ij} are plane parameters and k_i are constants. In order to verify the linear independence of normal vectors, let:

$$\Delta = \begin{vmatrix} a_{11} & a_{12} & a_{13} \\ a_{21} & a_{22} & a_{23} \\ a_{31} & a_{32} & a_{33} \end{vmatrix} \qquad (7)$$

The normal vectors of the three planes are linearly independent if $\Delta \neq 0$ in which case the set of equations 6 has a unique solution that can be calculated using Cramer's rule (Pedoe, 1963):

$$x = \Delta_x/\Delta \qquad y = \Delta_y/\Delta \qquad z = \Delta_z/\Delta$$

where:

$$\Delta_x = \begin{vmatrix} k_1 & a_{12} & a_{13} \\ k_2 & a_{22} & a_{23} \\ k_3 & a_{32} & a_{33} \end{vmatrix}$$

$$\Delta_y = \begin{vmatrix} a_{11} & k_1 & a_{13} \\ a_{21} & k_2 & a_{23} \\ a_{31} & k_3 & a_{33} \end{vmatrix} \qquad (8)$$

$$\Delta_z = \begin{vmatrix} a_{11} & a_{12} & k_1 \\ a_{21} & a_{22} & k_2 \\ a_{31} & a_{32} & k_3 \end{vmatrix}$$

Every three planar faces of the model are intersected and the intersection point, if there is one, is stored as a vertex for each of the three faces.

4.2 Verification of vertices

Intersection of model faces may generate incorrect vertices. Figure 2(B) shows an example of an incorrect vertex generated from the intersection of three model faces. All generated vertices, therefore, have to be verified, in order to identify and remove incorrect ones. To identify incorrect vertices, two constraints are used as follows:

- *Constraint 1: A valid vertex lies either in or under any roof plane.*

Recall that each building part is assumed to have one of the three presumed roof types: flat, gable and hipped. For these building types, all model vertices lie either in or under any roof plane. This property allows us to verify model vertices and identify invalid ones. The verification is carried out by evaluating the function of the roof plane with the coordinates of the vertex of interest. This will result in zero if the vertex lies in the roof plane, otherwise the sign of the resulting value and the direction of the plane normal vector determines whether the vertex point is above or under the roof plane. Every vertex is verified against all roof planes and is removed if it is higher than any of roof planes.
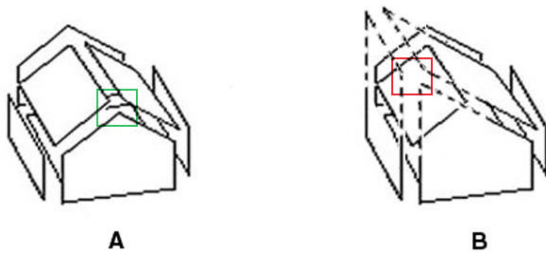

Figure 2: Intersection of model faces may generate incorrect vertices. A. A correct vertex; B. An incorrect vertex.

- *Constraint 2: A valid vertex projects on or inside the polygon of the ground plan.*

This constraint is based on the assumption that roof eaves do not overshoot walls. Figure 3 illustrates the procedure to verify whether a test point is on or inside a polygon. First vectors are formed from the test point to every polygon vertex and then cross product of every two adjacent vectors are computed. The test point is determined inside the polygon, if all computed cross products are non-zero and have the same sign. Otherwise if cross products are non-zero with different signs, the test point is outside the polygon. If any of the cross products is zero then the test point is determined to fall on a polygon side or on the extension of a polygon side. The distinction between the two cases is made by checking the dot product of the corresponding two vectors (which have a zero cross product). For a point on a side of the polygon, one of the cross products is zero and the corresponding dot product is negative, while for a point on the extension of the polygon side the dot product is positive (figure 3).
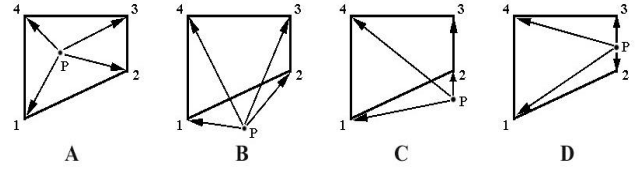
$\vec{V_1}$	$\vec{V_2}$	**A**	**B**	**C**		**D**	
		$\vec{V_1} \times \vec{V_2}$	$\vec{V_1} \times \vec{V_2}$	$\vec{V_1} \times \vec{V_2}$	$\vec{V_1} \circ \vec{V_2}$	$\vec{V_1} \times \vec{V_2}$	$\vec{V_1} \circ \vec{V_2}$
P1	P2	+	-	-	-	+	+
P2	P3	+	+	0	+	0	-
P3	P4	+	+	+	+	+	+
P4	P1	+	+	+	+	+	+

$\times$: Cross Product

$\circ$: Dot Product

Figure 3: Four possible positions of a point with respect to a polygon. A. Point inside the polygon: all cross products are non-zero and have the same sign; B. Point outside the polygon: cross products are non-zero but have different signs; C. Point on the extension of a polygon side: a zeros cross product with a positive dot product of the corresponding vectors; D. Point on the polygon side: a zero cross product but the dot product of the corresponding vectors is negative.

A correct vertex is one that satisfies both constraints. An incorrect vertex will fail to satisfy one or both constraints and will be removed from corresponding planar faces.

4.3 Sorting of vertices

For graphical visualization of the reconstructed model, vertices of each planar face must be given in order. To sort vertices a simple algorithm is used, which is based on forming vectors from the centre of gravity of vertices to each vertex and finding the angle between each vector and a starting vector (figure 4). The angle between vectors $\vec{u}$ and $\vec{v}$ is given by the dot product:

$$\cos(\boldsymbol{a}) = \frac{\vec{u} \circ \vec{v}}{|\vec{u}||\vec{v}|} \qquad (9)$$

Since cosine function returns the same value for $\pm\boldsymbol{a}$, the sign of the cross product between the two vectors is used to determine the direction of the angle. The algorithm starts with an arbitrary vertex and sorts other vertices with respect to the angle of their

vectors with the starting vector. The details of the algorithm is as follows:

Algorithm: Sort vertices
- Select an arbitrary vertex as the starting vertex;
- Find the center of gravity of remaining vertices;
- Form vectors from the center of gravity to each vertex;
- Compute the angle between each vector and the starting vector (eq. 9);
- Find the sign of the cross product of each vector and the starting vector;
- For any vector with a negative sign of the cross product change the angle a to $2p - a$.
- Sort the vertices with respect to their angles.

Sorted vertices of model faces form the planar patches. The generic polyhedral model is reconstructed once all its planar patches are formed.
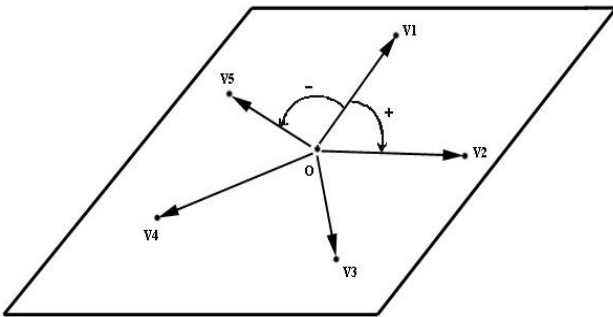
Figure 4: sorting the vertices of a planar face.

5. EXPERIMENTAL RESULTS

The image data used in the experiment is an orthorectified aerial image of 0.5m ground resolution acquired in RGB and NIR channels. Figure 5 shows the RGB image of the selected scene. Height data consists of a last echo DSM and a DTM in regular grid format with 1.0m resolution acquired using LIDAR (light detection and ranging) system. Figure 6 and figure 7 depict the DSM and the DTM respectively in grey levels where a brighter level stands for a higher altitude. Ground plans of the buildings in the scene were manually digitised from the image data and are shown in figure 8. Using the information in red and near infrared channels the NDVI measure was computed for each image pixel. The resulting NDVI map is shown in figure 9 where high NDVI values (vegetation pixels) are depicted in yellow and red colours.

Buildings were localized in the image and the split-and-merge process was applied to localized areas to reconstruct the roof planes. Image regions with NDVI values higher than 0.35 were identified as vegetation and were removed from the process. Figure 10 shows the results of the split-and-merge process as applied on the images of the three buildings in the scene. As can be seen in figure 10(B), the initial segmentation results in undergrown and overgrown regions in all cases. Figure 10(C), however, shows that these undergrown and overgrown regions are successfully split and merged respectively.

Figure 5: Colour aerial image of the selected scene.
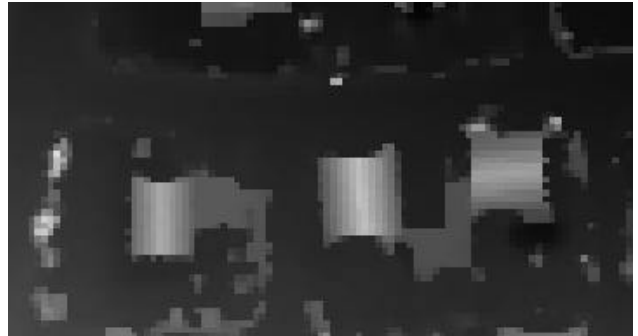

Figure 6: The DSM of the selected scene.
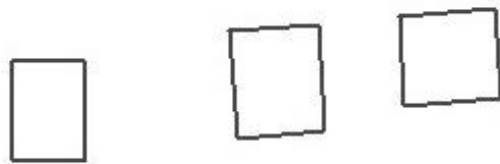

Figure 7: The DTM of the selected scene.

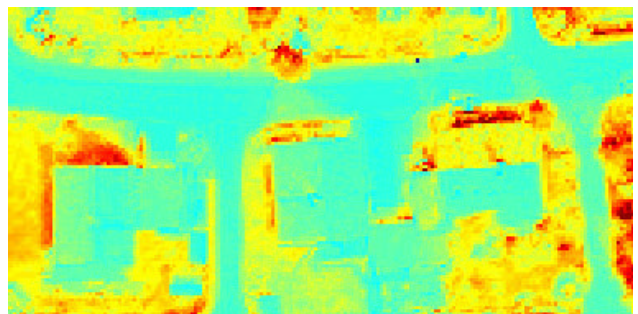Figure 8: The ground plans manually digitised from the image.

Figure 9: The NDVI map computed from image data in red and infrared channels.

The plane patch reconstruction technique was applied to parametric forms of roof planes computed in split-and-merge process and wall planes reconstructed upon ground plans. Figure 11 shows the generic polyhedral models reconstructed by assembling plane patches.
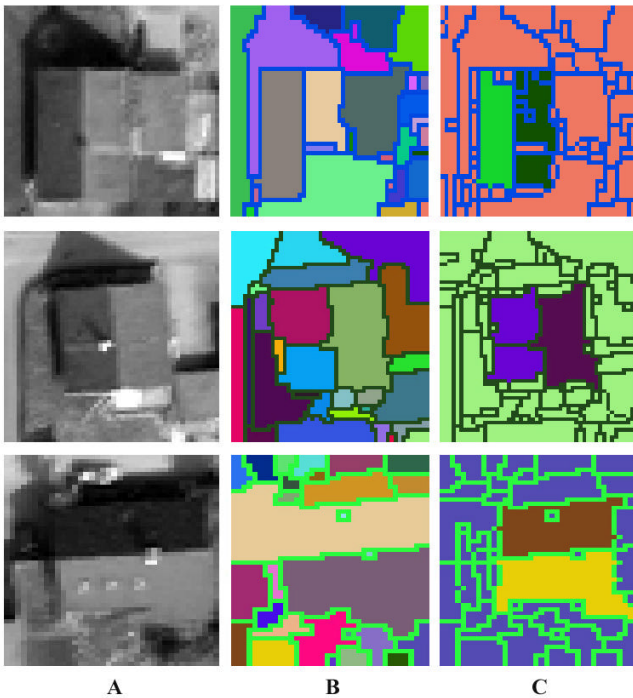

Figure 10: Results of the split-and-merge process for reconstruction of roof planes. A. Original images; B. Initial segmentations; C. Reconstructed roofs shown as image regions.
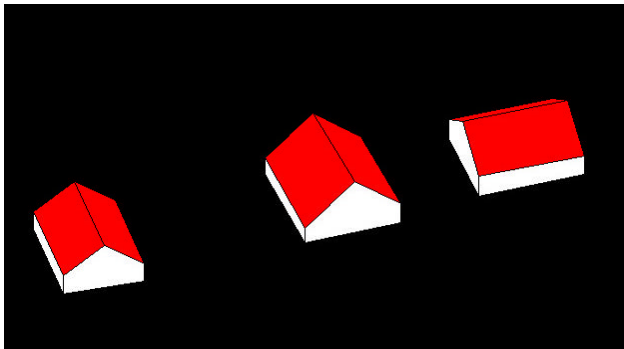

Figure 11: The reconstructed models.

6. CONCLUSION

A framework for fusion of image data, height data and 2D ground plans was presented in this paper. This fusion framework was used in an approach to automated detection and reconstruction of buildings. The relative simplicity of this approach suggests that fusing data from multiple sources can greatly reduce the complexity of the problem. Using generic models is advantageous since a larger number of buildings can be modelled. Nevertheless, successful reconstruction of generic models heavily depends on the results of detection. This is because these models are not sufficiently specific and other objects might as well be reconstructed as buildings. In this approach, however, detection of buildings using ground plans and height data is straightforward and guarantees that other objects will not be reconstructed as buildings.

The focus in the present work was on the reconstruction of simple roof types. Future research will target more complex roof types by adopting a CSG modelling scheme. This will concern finding all possible ways to partition the ground plan and select the correct one based on the number, parameters and attributes of reconstructed roof planes. Building parts will then be reconstructed using the approach described in this paper.

REFERENCES

Ameri, B., 2000. Automatic recognition and 3D reconstruction of buildings from digital imagery. PhD Thesis, Stuttgart University, Stuttgart, 110 pp.

Baillard, C., Schmid, C., Zisserman, A. and Fitzgibbon, A., 1999. Automatic line matching and 3D reconstruction of buildings from multiple views, ISPRS conference on automatic extraction of GIS objects from digital imagery, IAPRS Vol.32, Part 3-2W5, pp. 69-80.

Bignone, F., Henricsson, O., Fua, P. and Stricker, M., 1996. Automatic extraction of generic house roofs from high resolution aerial imagery, ECCV '96: 4th European Conference on Computer Vision, Cambridge, UK, April 15-18, pp. 85-96.

Brunn, A. and Weidner, U., 1997. Extracting buildings from digital surface models, ISPRS Workshop on 3D Reconstruction and Modelling of Topographic Objects, Stuttgart, pp. 27-34.

Cord, M., Jordan, M. and Cocquerez, J.-P., 2001. Accurate building structure recovery from high resolution aerial imagery. Computer Vision and Image Understanding, 82: 138-173.

Dang, T., Jamet, O. and Maitre, H., 1994. Applying perceptual grouping and surface models to the detection and stereo reconstruction of building in aerial imagery. In: H. Ebner, C. Heipke and K. Eder (Editors), ISPRS Symposium on Spatial Information from Digital Photogrammetry and Computer Vision, Munich, pp. 165-172.

Fischer, A. et al., 1998. Extracting buildings from aerial images using hierarchical aggregation in 2D and 3D. Computer Vision and Image Understanding, 72(2): 185-203.

Fischler, M.A. and Bolles, R.C., 1981. Random sample consensus: a paradigm for model fitting with applications to image analysis and automated cartography. Communications of the ACM, 24(6): 381-395.

Fua, P. and Hanson, A.J., 1991. An optimization framework for feature extraction. Machine vision and applications(4): 59-87.

Haala, N. and Anders, K., 1996. Fusion of 2D GIS and image data for 3D building reconstruction, International Archives of Photogrammetry and Remote Sensing, vol. XXXI, Part B3, pp. 285– 290.

Haala, N. and Brenner, C., 1998. Interpretation of urban surface models using 2D building information. Computer Vision and Image Understanding, 72(2): 204-214.

Henricsson, O., 1998. The Role of Color Attributes and Similarity Grouping in 3-D Building Reconstruction. Computer Vision and Image Understanding, 72(2): 163-184.

Henricsson, O. and Baltsavias, E., 1997. 3-D building reconstruction with ARUBA: A qualitative and quantitative evaluation. In: A. Gruen, E. Baltsavias and O. Henricsson (Editors), Automatic extraction of man-made objects from aerial images(II). Birkhauser Verlag, Basel, pp. 65-76.

Herman, M. and Kanade, T., 1986. Incremental reconstruction of 3D scenes from multiple complex images. Artificial Intelligence(30): 289-341.

Huertas, A., Lin, C. and Nevatia, R., 1993. Detection of buildings from monocular views of aerial scenes using perceptual organization and shadows, ARPA image understanding workshop, Washington, DC, pp. 253-260.

Jaynes, C., Riseman, E. and Hanson, A., 2003. Recognition and reconstruction of buildings from multiple aerial images. Computer Vision and Image Understanding, 90(1): 68-98.

Jibrini, H., Paparoditis, N., Pierrot-Desseilligny, M. and Maître, H., 2000. Automatic building reconstruction from very high resolution aerial stereopairs using cadastral ground plans, 19th ISPRS Congress, Amsterdam, The Netherlands.

Kolbe, T.H., 1999. Identifikation und Rekonstruktion von Gebäuden in Luftbildern mittels unscharfer Constraints. PhD Thesis, University of Vechta, Vechta, 149 pp.

Lin, C., Huertas, A. and Nevatia, R., 1995. Detection of buildings from monocular images. In: A. Gruen, O. Kuebler and P. Agouris (Editors), Automatic extraction of man-made objects from aerial and space images. Birkhauser Verlag, Basel, pp. 125-134.

Lin, C. and Nevatia, R., 1996. Buildings detection and description from monocular aerial images, ARPA Image Understanding Workshop, Palm Springs, CA.

Maas, H.G., 1999. Closed solutions for the determination of parametric building models from invariant moments of airborne laserscanner data, ISPRS Conference on Automatic Extraction of GIS Objects from Digital Imagery, Munich, pp. 193-199.

Moons, T., Frere, D., Vandekerckhove, J. and Van Gool, L., 1998. Automatic modeling and 3D reconstruction of urban house roofs from high resolution aerial imagery, European Conference on Computer Vision, Freiburg, Germany, pp. 410-425.

Nevatia, R., Lin, C. and Huertas, A., 1997. A system for building detection from aerial images. In: A. Gruen, E. Baltsavias and O. Henricsson (Editors), Automatic extraction of man-made objects from aerial images (II). Birkhauser Verlag, Basel, pp. 77-86.

Pasko, M. and Gruber, M., 1996. Fusion of 2D GIS data and aerial images for 3D building reconstruction, International Archives of Photogrammetry and Remote Sensing, vol. XXXI, Part B3,, pp. 461-468.

Pedoe, D., 1963. A geometric introduction to linear algebra. Wiley, New York, 224 pp.

Rottensteiner, F. and Jansa, J., 2002. Automatic extraction of buildings from LIDAR data and aerial images, International Archives of Photogrammetry and Remote Sensing, Volume XXXIV / 4, pp. 569-574.

Rousseeuw, P.J. and Leroy, A.M., 1987. Robust regression and outlier detection. John Wiley & Sons, New York, 329 pp.

Shufelt, J. and McKeown, D., 1993. Fusion of monocular cues to detect man-made structures in aerial imagery. CVGIP: Image Understanding, 57(3): 307-330.

Soille, P., 1999. Morphological image analysis: principles and applications. Springer, Berlin, 316 pp.

Suveg, I. and Vosselman, G., 2004. Reconstruction of 3D building models from aerial images and maps. ISPRS Journal of Photogrammetry and Remote Sensing, 58: 202-224.

Vincent, L. and Soille, P., 1991. Watersheds in digital spaces: an efficient algorithm based on immersion simulations. IEEE transactions on pattern analysis and machine intelligence, 13(6): 583-598.

Vosselman, G., 1999. Building reconstruction using planar faces in very high density height data, ISPRS Conference on Automatic Extraction of GIS Objects from Digital Imagery, Munich, pp. 87-92.

Weidner, U. and Forstner, W., 1995. Towards automatic building extraction from high resolution digital elevation models. ISPRS Journal of Photogrammetry and Remote Sensing, 50(4): 38-49.